THE JOURNAL OF COMPARATIVE NEUROLOGY 499:732–744 (2006)

Two Optic Flow Pathways from the Pretectal Nucleus Lentiformis Mesencephali to the Cerebellum in Pigeons (*Columba livia*)

JANELLE M.P. PAKAN[1] AND **DOUGLAS R.W. WYLIE**[1,2]*
[1]Division of Neuroscience, University of Alberta, Edmonton, Alberta, Canada T6G 2E9
[2]Department of Psychology, University of Alberta, Edmonton, Alberta, Canada T6G 2E9

ABSTRACT

Neurons in the pretectal nucleus lentiformis mesencephali (LM) are involved in the analysis of optic flow. LM provides mossy fiber inputs to folia VI–VIII of the posterior cerebellum and IXcd of the vestibulocerebellum. Previous research has shown that the vestibulocerebellum is involved in visual-vestibular integration supporting gaze stabilization. The function of folia VI–VIII in pigeons is not well understood; however, these folia receive input from a tectopontine system, which is likely involved with analyzing local motion as opposed to optic flow. We sought to determine whether the mossy fiber input from LM to IXcd differs from that to VI–VIII. Fluorescent retrograde tracers were injected into these folia, and the pattern of labeling in LM was observed. Large multipolar neurons were labeled throughout the rostrocaudal extent of LM. There was a clear mediolateral difference: 74.3% of LM neurons projecting to IXcd were located in the lateral subnucleus of LM (LMl), whereas 73.8% of LM neurons projecting to VI–VIII were found in medial LM (LMm). This suggests that the subnuclei of LM have differing roles. In particular, the LMl-IXcd pathway is involved in generating the optokinetic response. We suggest that the pathway from LMm to VI–VIII is integrating optic flow and local motion to support various oculomotor and visuomotor behaviors, including obstacle avoidance during locomotion. J. Comp. Neurol. 499:732–744, 2006. © 2006 Wiley-Liss, Inc.

Indexing terms: optokinetic; optic flow; vestibulocerebellum; avian cerebellum; fluorescent tracers; oculomotor cerebellum

As organisms move through their environment, optic flow occurs across the retina (Gibson, 1954). Optic flow subserves many behaviors: control of posture and locomotion, determination of heading, generation of compensatory movements, and navigation (Lee and Lishman, 1977; Simpson, 1984; Lappe and Rauschecker, 1994; Bardy et al., 1999; Srinivasan et al., 1999; O'Brien et al., 2001; Warren et al., 2001). Optic flow is analyzed by retinal-recipient nuclei in the accessory optic system (AOS; Simpson, 1984; Giolli et al., 2006) and pretectum (Simpson et al., 1988; Gamlin, 2006). In birds, this pretectal nucleus is known as the lentiformis mesencephali (LM), the homologue of the mammalian nucleus of the optic tract (NOT; Collewijn, 1975b; Hoffmann and Schoppmann, 1975; McKenna and Wallman, 1985). The nucleus of the basal optic root (nBOR) of the avian AOS is the homolog of the terminal nuclei of the mammalian AOS (Simpson, 1984; Giolli et al., 2006).

LM is a retinal-recipient structure that has been divided into medial and lateral subnuclei (LMm and LMl, respectively) based on cytoarchitecture (see also Gottlieb and McKenna, 1986; Gamlin and Cohen, 1988a). LM neurons respond best to moving large-field visual stimuli (i.e., optic flow; McKenna and Wallman, 1985; Winterson and

---

Grant sponsor: Canadian Institute for Health Research (CIHR); Grant numberr: 69013 (to D.R.W.W.); Grant sponsor: Natural Sciences and Engineering Research Council of Canada (NSERC); Grant number: 170363 (to D.R.W.W.); Grant sponsor: Canada Research Chairs Program.

*Correspondence to: Douglas Wong-Wylie, PhD, Department of Psychology, University of Alberta, Edmonton, Alberta Canada T6G 2E9. E-mail: dwylie@ualberta.ca

Received 19 December 2005; Revised 12 April 2006; Accepted 29 May 2006

DOI 10.1002/cne.21108

Brauth, 1985; Wylie and Crowder, 2000) and have been explicitly implicated in generation of the optokinetic response (Gioanni et al., 1983; Simpson et al., 1988). In pigeons, the efferent projections of LM include ipsilateral projections to the medial column of the inferior olive (mcIO), nBOR, parts of the anterior dorsal thalamus, and structures along the midline in the mesencephalon (Clarke, 1977; Gamlin and Cohen, 1988b; Wild, 1989; Wylie et al., 1998a, 1999; Wylie, 2001; Pakan et al., 2006). In addition, neurons in LM provide a bilateral mossy fiber projection to folia VI–VIII and IXcd. Together, folia IXcd and X make up the vestibulocerebellum, but X does not receive input from LM (Clarke, 1977; Brecha et al., 1980; Gamlin and Cohen, 1988b; Pakan et al., 2006). The vestibulocerebellum (uvula, nodulus, and flocculus) is involved in generating compensatory eye movements (Ito et al., 1974; Miles and Lisberger, 1981; Simpson, 1984; Waespe and Henn, 1987; Nagao et al., 1991; Wylie et al., 1998b). In contrast, the function of folia VI–VIII in pigeons has not been extensively investigated; however, these folia receive input from a tectopontine system (Clarke, 1977), which is implicated in avoidance behavior (Hellmann et al., 2004). In mammals, folia VI–VIII, in particular folium VII, are referred to as the “oculomotor vermis” and have been linked to saccades and pursuit eye movements (for review see Voogd and Barmack, 2006).

Previously we have shown that there are some differences with respect to the projection of LMm and LMl: the projection to nBOR and preoculomotor structures along the midline of the mesencephalon is primarily from LMl as opposed to LMm (Pakan et al., 2006). The aim of the present study was to determine whether the mossy fiber input from LM to folium IXcd differs from that to folia VI–VIII. We injected fluorescent retrograde tracers into these folia and observed the pattern of labeling in LM and throughout the brain.

MATERIALS AND METHODS

The methods reported herein conformed to the guidelines established by the Canadian Council on Animal Care and were approved by the Biosciences Animal Care and Policy Committee at the University of Alberta. Five silver king and homing pigeons (*Columba livia*), obtained from a local supplier, were anesthetized by intramuscular injection of a ketamine (65 mg/kg)/xylazine (8 mg/kg) cocktail, with supplemental doses administered as necessary. Animals were placed in a stereotaxic device with pigeon ear bars and a beak bar adapter so that the orientation of the skull conformed to the atlas of Karten and Hodos (1967). To access folia VI, VII, and VIII, bone was removed from the dorsomedial surface of the cerebellum, lateral to the midsagittal sinus. To access the flocculus, the bone surrounding the semicircular canals was removed, because the dorsal surface of the flocculus (folium IXcd) lies within the radius of the anterior semicircular canal. The dura was removed, and a glass micropipette (4–5 μm tip diameter) containing 2 M NaCl was advanced into the cerebellum with a hydraulic microdrive (Fredrick Haer & Co.). This allowed extracellular recordings to be made from Purkinje cell complex spike activity, and the depth of the granular layer of the targeted folium was determined. Once the desired depth was established, the recording electrode was replaced with a micropipette (tip diameter 20–30 μm) containing green or red fluorescent latex microspheres (Lumafluor Corp., Naples, FL). The red and green latex microspheres are retrograde tracers that fluoresce under rhodamine and fluorescein isothiocyanate (FITC) filters, respectively. The tracers were pressure injected by using a Picospritzer II (General Valve Corporation; 40 psi, 100 msec duration/puff). After surgery, the craniotomy was filled with bone wax and the wound su-

---

Abbreviations

AOS	accessory optic system
Au	auricle
Cb	cerebellum
CE	external cuneate nucleus
CP	posterior commisure
dl	dorsal lamella of the inferior olive
DLP	posterior dorsolateral nucleus of the thalamus
FLM	medial longitudinal fasiculus
FRL	lateral mesencephalic reticular formation
FRM	medial mesencephalic reticular formation
GCt	substantia grisea centralis
GLv	ventral leaflet of the lateral geniculate nucleus
GT	tectal gray
Hy	hypothalamus
I	folium I of the cerebellum
ICo	nucleus intercollicularis
Imc	nucleus isthmi, pars magnocellularis
IPS	nucleus interstitiopretectosubpretectalis
IS	interstitial nucleus (of Cajal)
IXcd	folium IXcd
LM	nucleus lentiformis mesencephali
LMl, LMm	nucleus lentiformis mesencephali, pars lateralis, pars medialis
LP	lateral pontine nuclei
LPC	nucleus laminaris precommisuralis
mcIO	medial column of the inferior olive
MLd	lateral mesencephalic nucleus, pars dorsalis
MP	medial pontine nuclei
MST	middle superior temporal area
nBOR	nucleus of the basal optic root
nBORd	nucleus of the basal optic root, pars dorsalis
nBORp	nucleus of the basal optic root, proper
NOT	nucleus of the optic tract
nVI	nucleus of the sixth cranial nerve (abducens)
NVI	sixth cranial nerve (abducens)
nX	nucleus of the vagus nerve
NXII	twelfth cranial verve (hypoglossal nerve)
nXII	nucleus of the twelfth cranial verve (hypoglossal)
OS	superior olive
PPC	nucleus principalis precommisuralis
PST	tractus pretectosubpretectalis
PT	pretectal nucleus
R	raphe
Rt	nucleus rotundus
Ru	nucleus ruber (red nucleus)
SCE/I	stratum cellulare externum/internum
SG	substantia gelatinosa Rolandi (trigemini)
Sop	stratum opticum
SP	nucleus subpretectalis
SpL	lateral spiriform nucleus
SpM	medial spiriform nucleus
TeO	optic tectum
TIO	tractus isthmoopticus
TrO	tractus opticus
TT	tectothalamic tract
TTD	descending trigeminal nerve nucleus and tract
VeS	superior vestibular nucleus
Vl	ventral lamella of the inferior olive
VTA	ventral tegmental area

tured. Birds were given an intramuscular injection of buprenorphine (0.012 mg/kg) as an analgesic.

After a recovery period of 2–3 days, the animals were deeply anesthetized with sodium pentobarbital (100 mg/kg) and immediately perfused with phosphate-buffered saline (0.9% NaCl, 0.1 M phosphate buffer). The brains were extracted, then flash-frozen in 2-methylbutane and stored at –80°C until sectioning. Brains were embedded in optimal cutting temperature medium, and 40-μm coronal sections were cut through the cerebellum, brainstem, and thalamus with a cryostat and mounted on electrostatic slides. Sections were viewed with a compound light microscope (Leica DMRE) equipped with the appropriate fluorescence filters (rhodamine and FITC). Images were acquired with a Retiga EXi FAST Cooled mono 12-bit camera (Qimaging, Burnaby, British Columbia, Canada) and analyzed with Openlab imaging software (Improvision, Lexington, MA). Images were adjusted in Adobe Photoshop to compensate for brightness and contrast.

Nomenclature

For the nomenclature of LM, we relied on Gamlin and Cohen (1988a,b), who divided the LM into a medial and a lateral subdivision (LMm, LMl, respectively). Both subnuclei contain large multipolar cells, which project to the vestibulocerebellum (Gottlieb and McKenna, 1986; Gamlin and Cohen, 1988b; Pakan et al., 2006). Continuous with the LMl at its lateral and caudal aspects is the tectal gray. The LMm, LMl, and rostral part of tectal gray all receive retinal input (Gamlin and Cohen, 1988a). The LMm is bordered medially by the nucleus laminaris precommissuralis, a thin strip of cells that does not receive retinal input. Medial to the nucleus laminaris precommisuralis is the nucleus principalis precommissuralis, which is lateral to the nucleus rotundus (see Fig. 3E–I). In Nissl-stained sections and in fresh tissue viewed under the fluorescent microscope, the layers of the pretectum are relatively easy to distinguish, although the border between tectal gray and LMl can be difficult to localize. Previously the LMm was known as the LM magnocellularis (LMmc), and the LMl and tectal gray were included as the LM parvocellularis (LMpc; Karten and Hodos, 1967).

For the nomenclature of the subdivisions of the inferior olive, we relied on Arends and Voogd (1989). The inferior olive consists of a dorsal and a ventral lamella that are joined medially by the medial column of the inferior olive (mcIO). The mcIO projects topographically to the vestibulocerebellum (Wylie et al., 1999; Crowder et al., 2000). For the zonal projection of the ventral lamella and the dorsal lamella to folia VI–VIII, we also relied on Arends and Voogd (1989). For the nomenclature of the cerebellar folia, we used Karten and Hodos (1967).

As in mammals, the cerebellum in birds is highly foliated but is restricted to a vermis without hemispheres. Folia IXcd (uvula) and X (nodulus) make up the vestibulocerebellum. Larsell (1967) considered the lateral extensions of folium IXcd and X as the paraflocculus and flocculus, respectively. In recent years, we (Wylie and Frost, 1999; Winship and Wylie, 2003; Wylie et al., 2003a,b) have divided the vestibulocerebellum into flocculus, nodulus, and ventral uvula based on function and homology with mammals. Purkinje cells throughout the vestibulocerebellum respond to optokinetic stimulation (see, e.g., Wylie et al., 1993). In the lateral half of IXcd and X, they respond best to rotational stimuli about the vertical axis (rVA neurons) or a horizontal axis oriented 45° to the midline (rH45 neurons). These responses are essentially identical to those observed in the mammalian flocculus (Graf et al., 1988; Wylie and Frost, 1993). Thus, we consider these zones in the lateral half of both IXcd and X as the flocculus. In mammals, a similar phenomenon has occurred: parts of the cerebellum traditionally included in the ventral paraflocculus are now considered part of the “floccular region,” “lobe,” or “complex” (see Voogd and Barmack, 2006). In keeping with Larsell (1967), we refer to the medial half of folia IXcd and X as the “uvula” and “nodulus,” respectively.

RESULTS

Injection sites and retrograde labeling in the inferior olive

In all experimental animals, an injection of either red or green latex microspheres was made into folium IXcd, and an injection of an alternate color was made into one of folia VI (1), VII (3), or VIII (1). The topography of the projection from the subnuclei of the inferior olive to the cerebellar cortex has been well documented (Arends and Voogd, 1989; Lau et al., 1998; Wylie et al., 1999; Crowder et al., 2000; Pakan et al., 2005), so the pattern of retrograde labeling in the inferior olive served as a guide to verify the location and extent of the injection sites. Figure 1 shows a schematic of the olivocerebellar projections and zonal organization of the posterior vermis based on these aforementioned studies. Specifically, for injections in VI–VIII, retrograde labeling in the dorsal lamella of the inferior olive (see Fig. 4A,B) was indicative of an injection in zone A_1 and/or A_2, labeling in the ventral lamella of the inferior olive (Fig. 4C) was indicative of an injection in zone C, and labeling in the ventral strip of the mcIO was indicative of an injection in zones B or E. For the IXcd injections, labeling in the caudal half of the medial mcIO was indicative of injections in floccular zones 0 and 2 (rVA zones), whereas labeling in the rostral half of the medial mcIO was indicative of injections in floccular zones 1 and 3 (rH45 zones; Fig. 4B,C; Wylie et al., 1999; Pakan et al., 2005). Labeling in the lateral half of the mcIO (i.e., lateral to the twelfth cranial nerve) was indicative of injections in the translation areas in the medial half of folium IXcd (ventral uvula; Fig. 1A; Lau et al., 1998; Crowder et al., 2000). Figure 2 shows drawings of the locations and extent of the injection sites from all cases. Based on these data, the zonal location of each injection is indicated in Table 1.

In four cases (cases 1–4), injections into folium IXcd were made just below the surface of the exposed auricle, i.e., the flocculus (Fig. 2A–D), and retrograde labeling was abundant in the medial mcIO but absent in the lateral mcIO. In the remaining case (case 5), the injection in IXcd was more medial in the vestibulocerebellum; i.e., the uvula (Fig. 2E). Labeling was restricted to the lateral mcIO, indicating the injection spared the flocculus. A few cells were observed ipsilateral to the exposed side, indicating that the injection crossed the midline. All five injections in IXcd appeared confined to that folium, with the possible exception of case 2. In this case, there was some suggestion that the injection spread into the adjacent folium IXab, but there were no retrogradely labeled cells in the ventral or dorsal lamellae of the inferior olive.

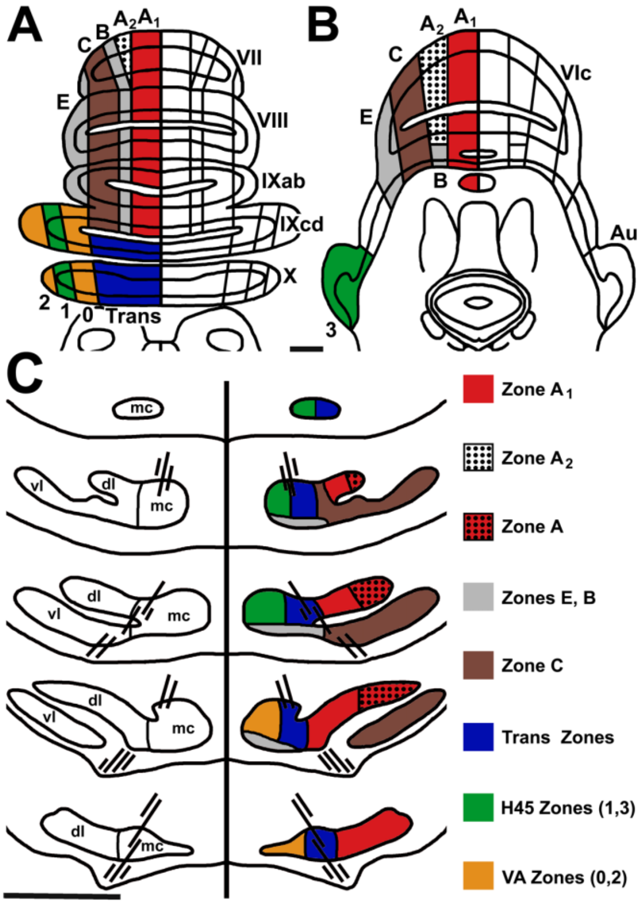

Fig. 1. Olivocerebellar zones in the pigeon. **A** and **B** show representations of coronal sections through the cerebellum (A, caudal; B, rostral). **C** shows coronal sections through the inferior olive (top = rostral). The parasaggital zones shown on the left side in A and B are color coded to correspond with the region of the inferior olive providing climbing fiber input. The organization of the zones in the vestibulocerebellum (folia IXcd and X) is based on Wylie and colleagues (Lau et al., 1998; Wylie et al., 1999; Crowder et al., 2000; Pakan et al., 2005). Zones 0–3 make up the flocculus and contain the rotation sensitive Purkinje cells (rVA and rH45 zones). The "trans" zone includes the nodulus (X) and ventral uvula (IXcd) and contains Purkinje cells responsive to translational optokinetic stimuli. Zones A–E are based on Arends and Voogd (1989). For abbreviations see list. Scale bars = 1 mm.

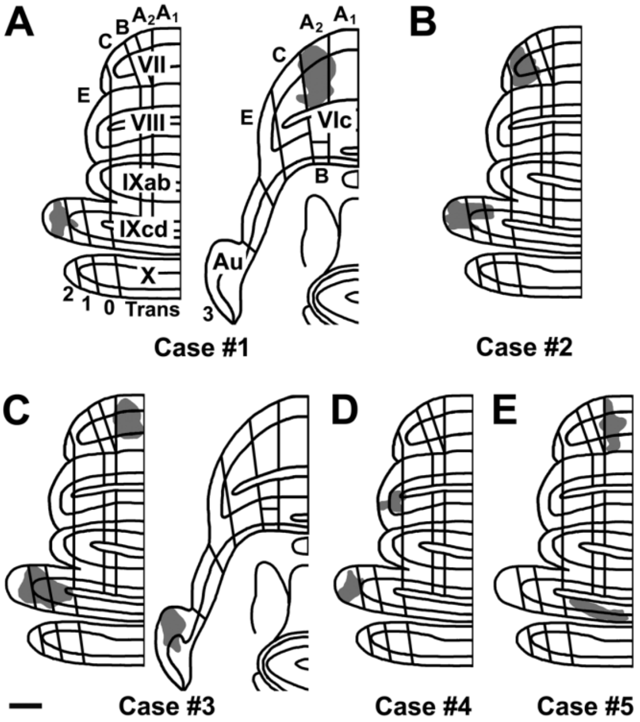

Fig. 2. Location and extent of injection sites in the cerebellum. **A–E** show representations of half coronal sections through the pigeon cerebellum, illustrating each injection site (gray shading) according to case number. Vertical lines through the folia represent climbing fiber projection zones, which are labeled in A (see also Fig. 1). Each case had two injection sites; one in folium IXcd and one in folia VI, VII, or VIII. Au, auricle. Scale bar = 1 mm.

Retrograde labeling in LM, nBOR, and other brain regions

Retrograde labeling was analyzed throughout the brain, focusing on several areas that project to folia VI–IXcd. Figure 3 shows selected tracings of coronal sections from case 3, illustrating retrograde labeling from injections (Fig. 3J) in VII (green) and IXcd (red). From caudally to rostrally, the main areas of interest include the inferior olive (Fig. 3A), the medial and lateral pontine nuclei (Fig. 3B), the nucleus of the basal optic root (nBOR; Fig. 3C), the medial spiriform nucleus (Fig 3D), and the LM (Fig. 3E–I). Surprisingly little labeling was seen in the ventral leaflet of the lateral geniculate nucleus, even though we have observed labeling in previous studies from injections of retrograde tracer into folium IX (Pakan et al., 2006). In all cases, only a few scattered cells were observed in caudolateral aspect of this nucleus. Retrogradely labeled cells were also found in the vestibular and cerebellar nuclei, particularly from the IXcd injections, but were not analyzed in any detail.

Labeled cells were observed in LM and nBOR from all injections (Fig. 4D–G; see also Fig. 3C, E-I). Overall, labeling in the nBOR was equally abundant on the contra- and ipsilateral sides (48% vs. 52%). Labeling in the LM was greater on the contralateral side (60% vs. 40%). In Table 1, the numbers of cells found in the contralateral nBOR and LM are indicated for each injection. Figure 5A shows a histogram of the relative percentage of cells labeled in the contralateral nBOR vs. LM averaged across all injections in IXcd (left) vs. injections in VI–VIII (right). Note that there was relatively more input to IXcd from nBOR compared with LM (60:40; see also Fig. 4D). However, the input to VI–VIII was much heavier from LM compared with nBOR; the projection from nBOR to VI–VIII was sparse (Table 1; see also Fig. 3C).

The drawings in Figure 3E–I show the distribution of retrograde labeling in the contralateral LM from case 3. Figure 4E–G shows fluorescent photomicrographs of retrograde labeling in the contralateral LM from case 2 (E,F) and case 5 (G). These images represent the typical pattern of labeling observed in LM: retrogradely labeled cells from folia VI–VIII injections were found mainly in LMm, whereas the input to IXcd was largely from LMl. Averaged

TABLE 1. Summary of the Injection Site Locations and Retrograde Labeling in the Medial and Lateral Subnuclei of the Pretectal Nucleus Lentiformis Mesencephali (LMm. LMl) and Nucleus of the Basal Optic Root (nBOR) Contralateral to the Injection Site

			No. of cells labeled from IXcd injections			No. of cells labeled from VI–VIII injections		
Case	IXcd injection	VI–VIII injection	nBOR	LMm	LMl	nBOR	LMm	LMl
1	Flocculus zone 2	VI (red) zone A_2	35	6	20	69	173	86
2	Flocculus zones 1, 2	VII (green) zone C	111	63	45	35	344	53
3	Flocculus zones 0-3	VII (green) zone A_1	133	21	96	12	41	22
4	Flocculus zone 2	VIII (red) zone E	66	0	17	28	54	21
5	Uvula all zones	VII (red) zone A_1	503	109	263	2	29	8
Total			848	215	518	146	641	190

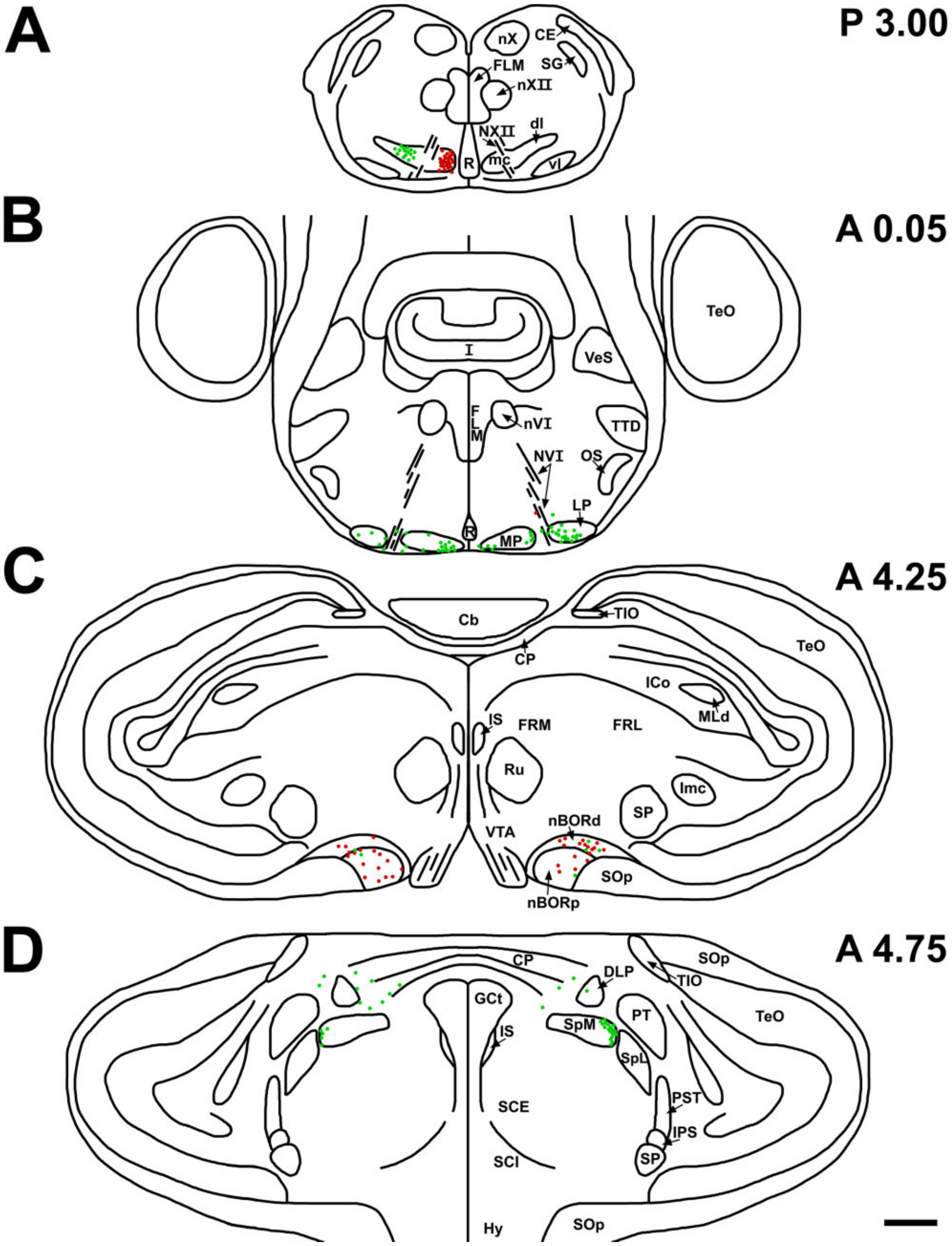

Fig. 3. Distribution of retrograde labeling from injections into folium IXcd and folium VII (case 3). **A–D** show tracings of coronal sections, caudal to rostral, through the inferior olive, the pontine nuclei, the nucleus of the basal optic root, and the spiriform nuclei, respectively. The approximate anterior-posterior locations according to the atlas of Karten and Hodos (1967) are listed at right. The red (folium IXcd projecting cells) and green (folium VII projecting cells) dots represent retrogradely labeled cells resulting from injections shown in J. **E–I** show tracings, caudal to rostral, approximately 160 μm apart, through the contralateral LM. The dark and light gray shading represents the lateral and medial subnuclei of LM, respectively. **J** shows a fluorescent image of the injection sites. The folia are outlined in white, and the white matter is shown as solid white. See list for abbreviations. Scale bars = 1 mm in D (applies to A–D); 1 mm in I (applies to E–I); 1 mm in J.

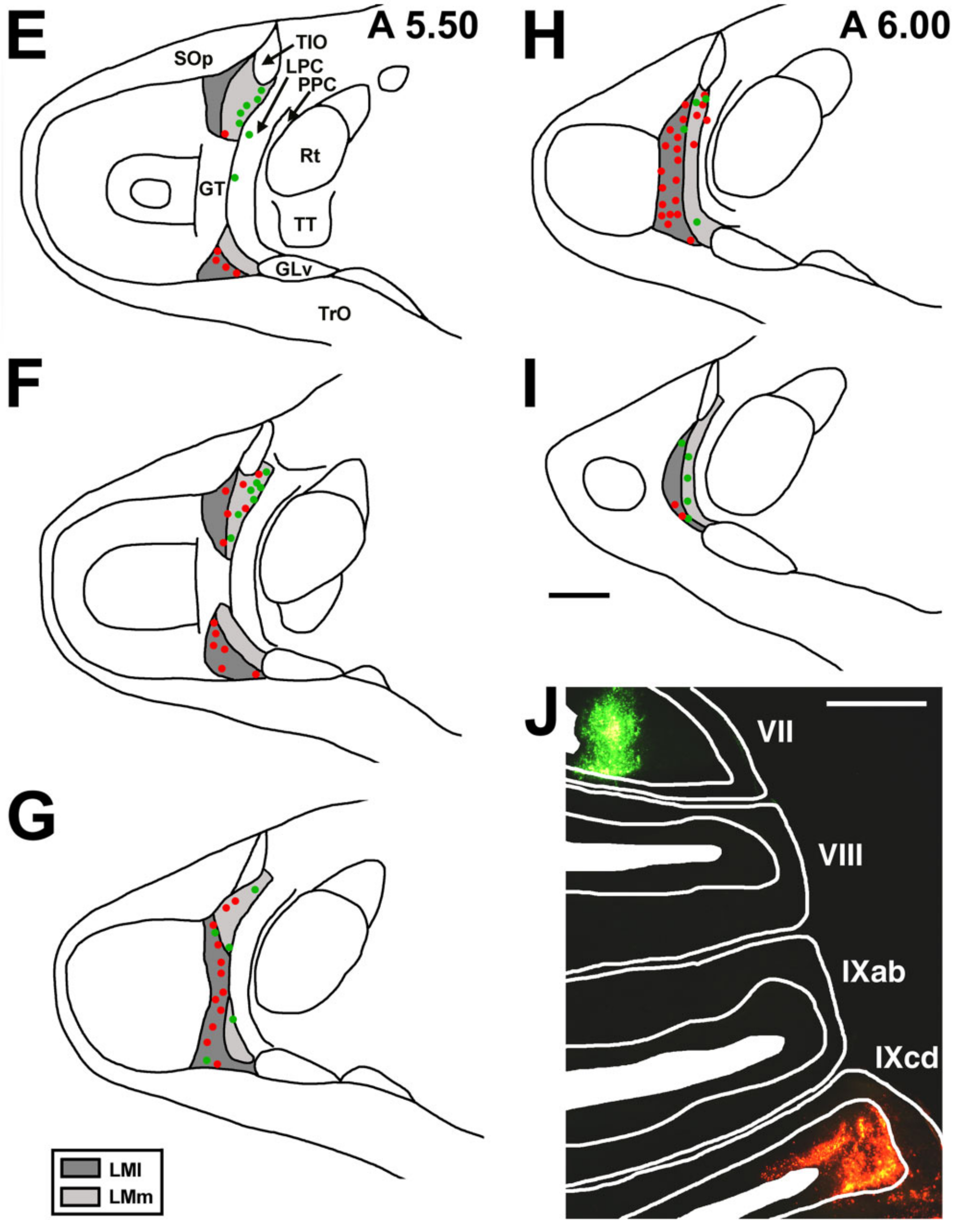

Figure 3 (Continued)

across all cases, 73.8% of retrogradely labeled neurons from injections into VI–VIII were in LMm, and the remaining 26.2% were in LMl. The opposite pattern of retrograde labeling was found for injections in folium IXcd: 74.3% of labeled cells were in LMl, and the remaining 25.7% were in LMm (Fig. 5B). In addition, there was also a dorsal-ventral difference in the distributions such that more cells from the injections in VI–VIII were labeled in the dorsal region of LM, and more cells from the IXcd injections were labeled in the ventral region of LM. This differential aspect of the distribution is particularly evident in the caudal regions of LM (see Fig. 3 E,F) and was present in all cases. Nine double-labeled LM cells were observed, and all were from case 2. As mentioned above, it was possible that the injection in IXcd for this case might have spread into IXab. Thus, with a possible few exceptions, individual LM neurons do not project to both IXcd and VI–VIII.

With respect to the retrograde labeling in nBOR (Figs. 3C, 4D), there was no apparent difference in the distribution of cells labeled from injections into IXcd vs. VI–VIII. Recall that comparatively few cells were labeled from the VI–VIII injections, but from all injections labeled cells were distributed throughout the nucleus, including the dorsal and the lateral extensions. In total, 10 double-labeled nBOR cells were found in four cases. Thus, few individual nBOR cells project to both IXcd and VI–VIII.

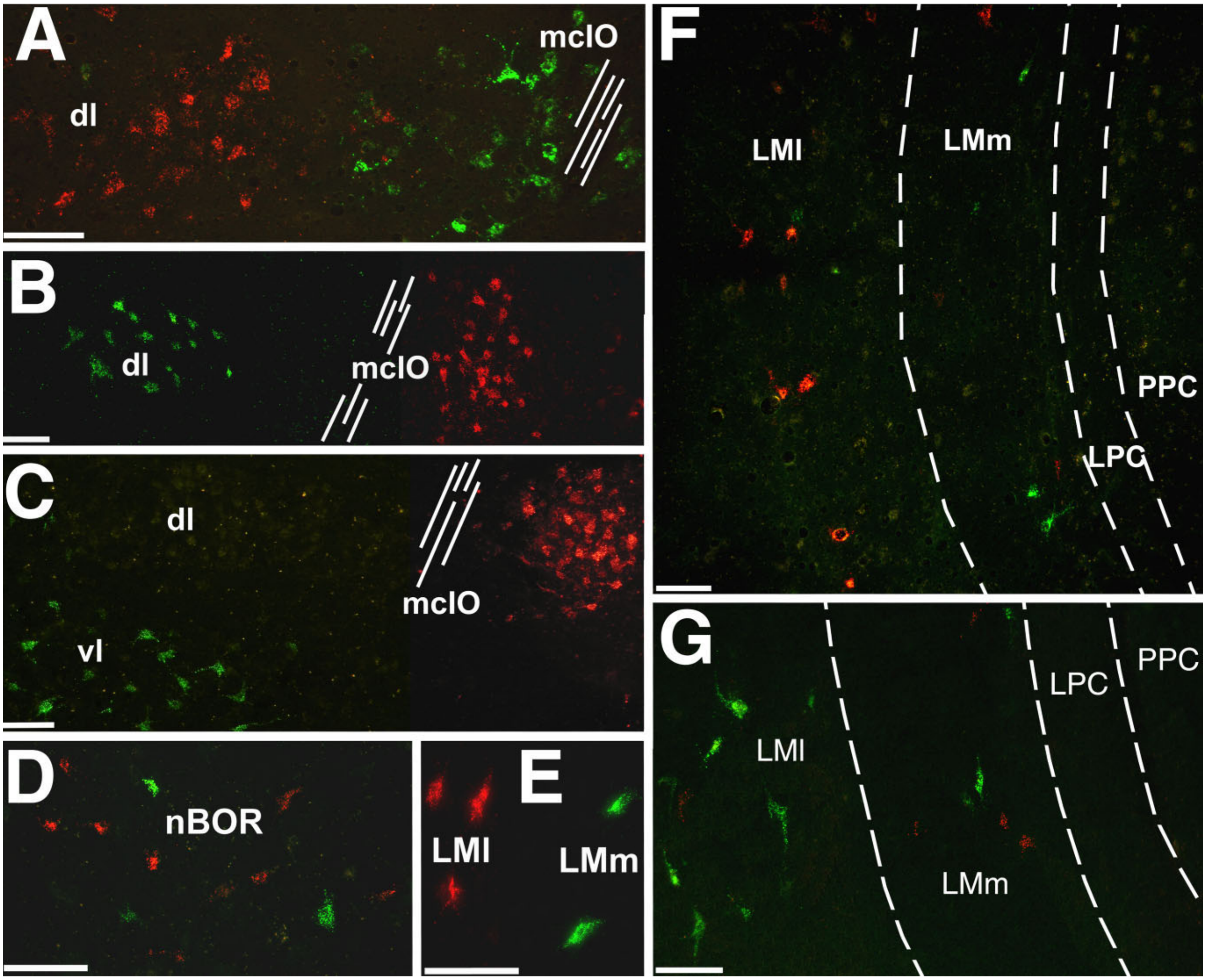

Fig. 4. Photomicrographs of retrograde labeling in the accessory optic system, pretectum, and inferior olive. **A–C:** Retrograde labeling in the inferior olive from cases 5, 3, and 2, respectively. The white lines highlight the genu of the hypoglossal nerve. Injections into folia VI–VIII labeled cells in the dorsal and ventral lamella of the inferior olive, and injections into folium IXcd labeled cells in the medial column of the inferior olive (mcIO). **D** shows labeled cells in the nucleus of the basal optic root (nBOR) from a green injection in VII and a red injection in IXcd (case 3). The distribution within nBOR was not observed to be different between injection regions; however, more nBOR cells were labeled from injections in folium IXcd of the vestibulocerebellum compared with folia VI–VIII injections. **E–G** show labeled cells in the nucleus lentiformis mesencephali (LM) from cases 2 (E,F; a green injection in VII and a red injection in the flocculus of IXcd) and 5 (G; a green injection in the uvula of IXcd and a red injection in VII). The dashed white lines represent the boarders of the subnuclei and surrounding areas. There was approximately three times more labeling observed in the lateral subnuclei of LM (LMl) compared with the medial subnuclei of LM (LMm) from injections into folium IXcd. Conversely, approximately three times more labeling was observed in LMm compared with LMl from injections into folia VI–VIII. LPC, nucleus laminaris precommisuralis; PPC, nucleus principalis precommisuralis. Scale bars = 100 μm.

Figure 6A–C shows photomicrographs of retrograde labeling in the pontine nuclei from injections into folia VII (cases 2 and 3). Heavy labeling was found throughout the medial and lateral pontine nuclei following injections into VI–VIII. This labeling was bilateral, but in general there was more labeling on the contralateral side. From the injections into VII, there was more labeling in the medial pontine nuclei compared with the lateral pontine nuclei. Retrograde labeling in the medial and lateral pontine nuclei was not observed from the flocculus injections, but a few cells were labeled from the uvula injection (see also Fig. 3B).

Figure 6D shows photomicrographs of retrogradely labeled cells in the medial spiriform nucleus from an injection into folia VII in case 3 (see also Fig. 3D). From all injections into VI–VIII, a strip of cells was labeled along the dorsolateral border of the medial spiriform nucleus. Diffuse labeling of large multipolar cells was also found dorsomedial to the medial spiriform nucleus. It was difficult to ascribe these to a specific nucleus, but they appeared to reside within the medial pretectal nucleus, the dorsolateral nucleus of the posterior thalamus, and/or the area pretectalis. There was no labeling in the medial spiriform nucleus from any IXcd injections.

DISCUSSION

For pigeons, we have shown that there is a topographic projection from the pretectal nucleus LM to the cerebellum. The projection to folium IXcd of the vestibulocerebellum arises mainly from LMl, whereas that to folia VI–VIII arises mainly from LMm. Previous electrophysical studies have not revealed a difference between LMl and LMm: both subnuclei process optic flow information (Winterson and Brauth, 1985; Crowder et al., 2003). Neurons in the avian LM have extremely large receptive fields (average = 60°) and exhibit direction selectivity in response to moving large-field stimuli. Most neurons prefer temporal to nasal motion in the contralateral visual field (McKenna and Wallman, 1985; Winterson and Brauth, 1985; Wylie and Crowder, 2000). Neurons with essentially identical properties have been found in the NOT (Collewijn, 1975a; Hoffmann and Schoppmann, 1981; Winterson and Brauth, 1985; Mustari and Fuchs, 1990). Previous lesion and stimulation studies of LM and NOT have emphasized their role in the optokinetic response (Gioanni et al., 1983; Cohen et al., 1992): lesions to LM or NOT markedly impair or abolish the optokinetic response to stimuli moving in the temporal to nasal direction. Whereas the LM has been linked only to the generation of the optokinetic response, studies suggest the NOT is involved in other behaviors, including pupillary constriction and convergence (“near” response; Buttner-Ennever et al., 1996b), smooth pursuit (Mustari and Fuchs, 1990; Ilg et al., 1993; Buttner-Ennever et al., 1996b; Yakushin et al., 2000), and saccades (Ballas and Hoffmann, 1985; Sudkamp and Schmidt, 1995; Schmidt, 1996; Price and Ibbotson, 2001).

Mossy fiber inputs to the posterior cerebellum

Similarly to the case in pigeons, a direct mossy fiber pathway from LM and nBOR to the cerebellum has been reported in turtles and fish, but not frogs (fish: Finger and Karten, 1978; turtle: Reiner and Karten, 1978; frogs: Montgomery et al., 1981). In mammals, there has been no report of a mossy fiber pathway from the NOT to the cerebellum, but a mossy fiber projection from the medial terminal nucleus of the AOS to the vestibulocerebellum has been reported in some species (chinchilla: Winfield et al., 1978; tree shrew: Haines and Sowa, 1985), but not others (cats: Kawasaki and Sato, 1980; rats and rabbits: Giolli et al., 1984). There is evidence of several indirect pathways from NOT to the cerebellum through which optic flow information can be conveyed. Most of the mossy fiber input to the vestibulocerebellum arises in the vestibular nuclei and the prepositus hypoglossi (Voogd et al., 1996; Ruigrok, 2003), but there are also projections originating in the reticular formation, raphe nuclei, and neurons located within and around the medial longitudinal fasciculus (Blanks et al., 1983; Sato et al., 1983; Gerrits et al., 1984; Langer et al., 1985; Voogd et al., 1996; Ruigrok, 2003). The NOT projects to many of these structures, including the vestibular nuclei, the medial and dorsolateral nuclei of the basilar pontine complex, the mesencephalic reticular formation, the prepositus hypoglossi, and the nucleus reticularis tegmenti pontis (Itoh, 1977; Terasawa et al., 1979; Cazin et al., 1982; Holstege and Collewijn, 1982; Giolli et al., 1984, 1985; Torigoe et al., 1986a,b; Giolli et al., 1988; for review see Simpson et al., 1988). Information from the NOT also reaches folium VII of the oculomotor vermis via the dorsal, medial, and dorsolateral pontine nuclei and the nucleus reticularis tegmenti pontis (Torigoe et al., 1986b; Yamada and Noda, 1987; Thielert and Thier, 1993; Voogd and Barmack, 2006).

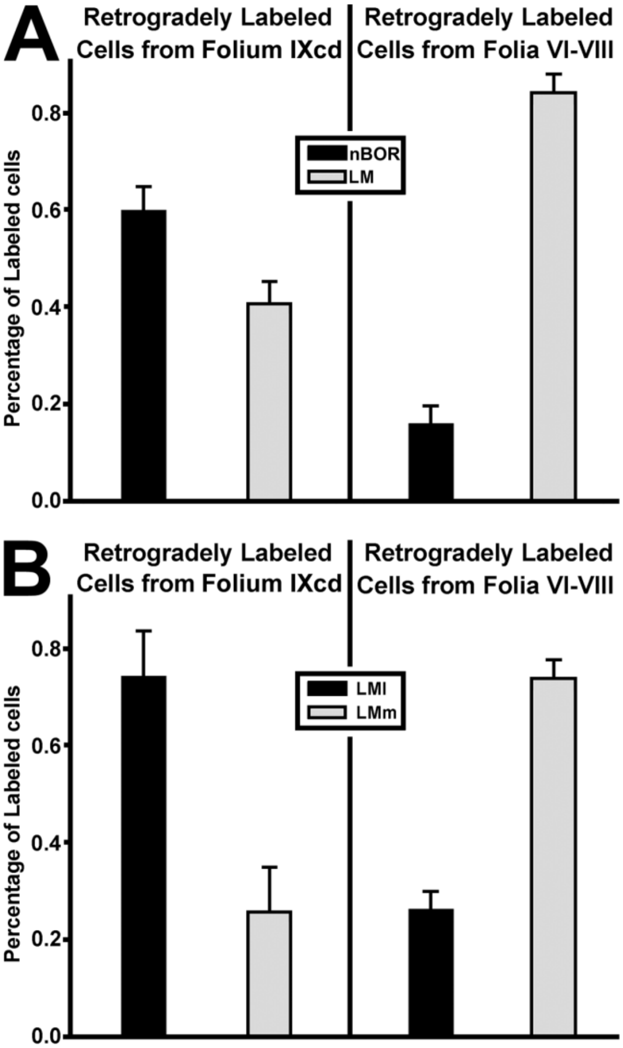

Fig. 5. Magnitude of labeling in the accessory optic system and pretectum from injections into folium IXcd vs. folia VI–VIII. **A** shows a histogram of the relative percentage of cells labeled in the contralateral nucleus of the basal optic root (nBOR; black bars) compared with the contralateral nucleus lentiformis mesencephali (LM; gray bars) averaged across all injections in folium IXcd (left) vs. injections in folia VI–VIII (right). A higher percentage of cells was labeled in nBOR from IXcd injections, and a higher percentage of cells was labeled in LM from VI–VIII injections. **B** shows a histogram of the relative percentage of cells in the contralateral lateral subnucleus of lentiformis mesencephali (LMl; black bars) and medial subnucleus of lentiformis mesencephali (LMm; gray bars) averaged across all injections in IXcd (left) vs. injections in VI–VIII (right). Most of the labeled neurons from injections into VI–VIII were in LMm. Conversely, most of the labeled neurons from injections into IXcd were in LMl.

Visual projections to the vestibulocerebellum and folia VI–VIII

Figure 7A shows a schematic of the connectivity from LM and nBOR to folium IXcd in pigeons. Included are mossy fiber connections (present study; Clarke, 1977; Bre-

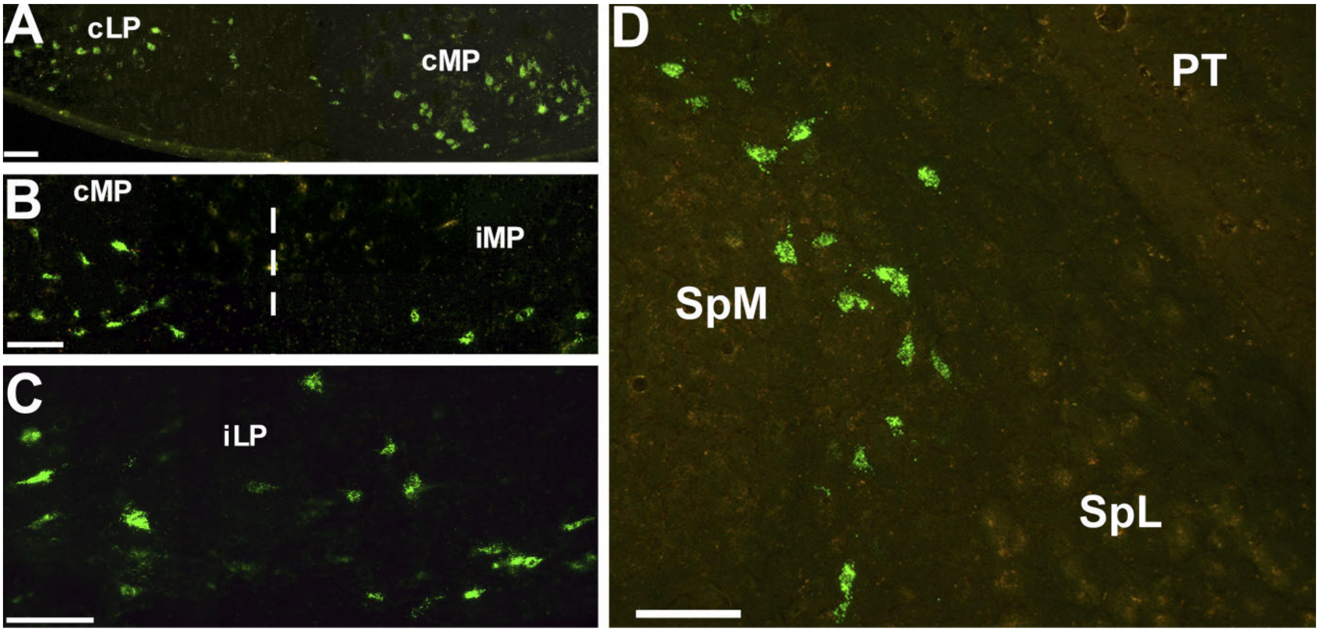

Fig. 6. Retrograde labeling in pontine nuclei and the medial spiriform nucleus. **A–C** show photomicrographs of retrograde labeling in the pontine nuclei from injections into folia VII (cases 2 and 3). Labeled cells can be seen throughout the pontine nuclei on the ipsilateral and contralateral side. There was more labeling in the medial pontine nucleus (MP) compared with the lateral pontine nucleus (LP) from folia VII injections (A). In general, there was more labeling observed in the contralateral pontine nuclei (B; the dashed line represents midline). **D** shows a photomicrograph of retrogradely labeled cells in the medial spiriform nucleus (SpM) from an injection into folium VII (case 3). From injections into folia VI–VIII, a specific and reliable distribution of labeling was seen in SpM, namely, a strip of cells found on the dorsolateral boarder of the nucleus. There was no labeling found in SpM from folium IXcd injections in any of the cases. i/cMP, ipsilateral/contralateral medial pontine nuclei; i/cLP ipsilateral/contralateral lateral pontine nuclei; SpL, lateral spiriform nucleus; PT, pretectal nucleus. Scale bars = 100 μm.

cha et al., 1980; Gamlin and Cohen, 1988b) and visual climbing fiber inputs (Arends and Voogd, 1989; Lau et al., 1998; Wylie et al., 1999; Crowder et al., 2000; Wylie, 2001). There is heavy mossy fiber input to folium IXcd from nBOR and LMl, but much less from LMm. Input from the pontine nuclei is minimal.

The climbing fiber pathway to the vestibulocerebellum arises from the mcIO, which receives topographic input from the LM and nBOR (Wylie, 2001). The connectivity of the optokinetic-olivovestibulocerebellum pathway is remarkably similar in mammals (Voogd et al., 1996; Voogd and Wylie, 2004). Furthermore, the zonal organization of the flocculus is strikingly similar in mammals and birds (Voogd and Wylie, 2004). Research in many species has shown that the flocculus is critical for integrating optokinetic, vestibular, and eye muscle proprioceptive information to control compensatory eye movements (Buttner-Ennever et al., 1996a,b; Buttner-Ennever and Horn, 1996; Buttner-Ennever, 2005). The optic flow input is critical for the modification of the VOR gain (see, e.g., Robinson, 1976; Zee et al., 1981; Ito et al., 1982; Nagao, 1983; Waespe and Cohen, 1983; Lisberger et al., 1984, 1994). The role of the ventral uvula and nodulus is not as clear as the flocculus. In a recent review, Voogd and Barmack (2006) concluded that the nodulus does not control eye movement per se but is involved in refining movement and postural reflexes.

Figure 7B shows a schematic of the input to folia VI–VIII in pigeons. The mossy fiber input is largely from LMm and weak from LMl and nBOR, and there is a heavy input from the pontine nuclei (medial and lateral) and the medial spiriform nucleus. In pigeons, the cerebellar projection from the pontine nuclei has been reported previously (Clarke, 1977). Karten and Finger (1976) reported that the medial spiriform nucleus projects to folia VIb–IXa of the cerebellum and that it receives afferents from the telencephalon. Given the fact that there is not a substantial corticopontocerebellar pathway in birds, these authors proposed that the medial spiriform nucleus was similar to a pontine nucleus in mammals insofar as it provides a pathway from the telencephalon to the cerebellum. However, little is known about the function of the medial spiriform nucleus.

In pigeons, the climbing fiber input to folia VI–VIII is from the dorsal and ventral lamellae of the inferior olive and is zonally organized (Arends and Zeigler, 1991). The information carried by these climbing fiber inputs to VI–VIII is unclear, and studies are wanting. Larsell (1967) suggested that folium VII is responsible for “visual power,” noting that this folium was large in raptors. Clarke (1974) recorded visual units in VI–VIII and suggested that they were of tectal origin. In the tectum, neurons respond to small moving stimuli or relative motion (Frost and Nakayama, 1983), and there is a heavy projection from the tectum to the medial and lateral pontine nuclei (Clarke, 1977). Albeit to a lesser degree, LM also projects to the pontine nuclei (Clarke, 1977; Gamlin and Cohen, 1988b). Thus, VI–VIII receives both optic flow information, from LMm, and local motion information, from a tectopontine system.

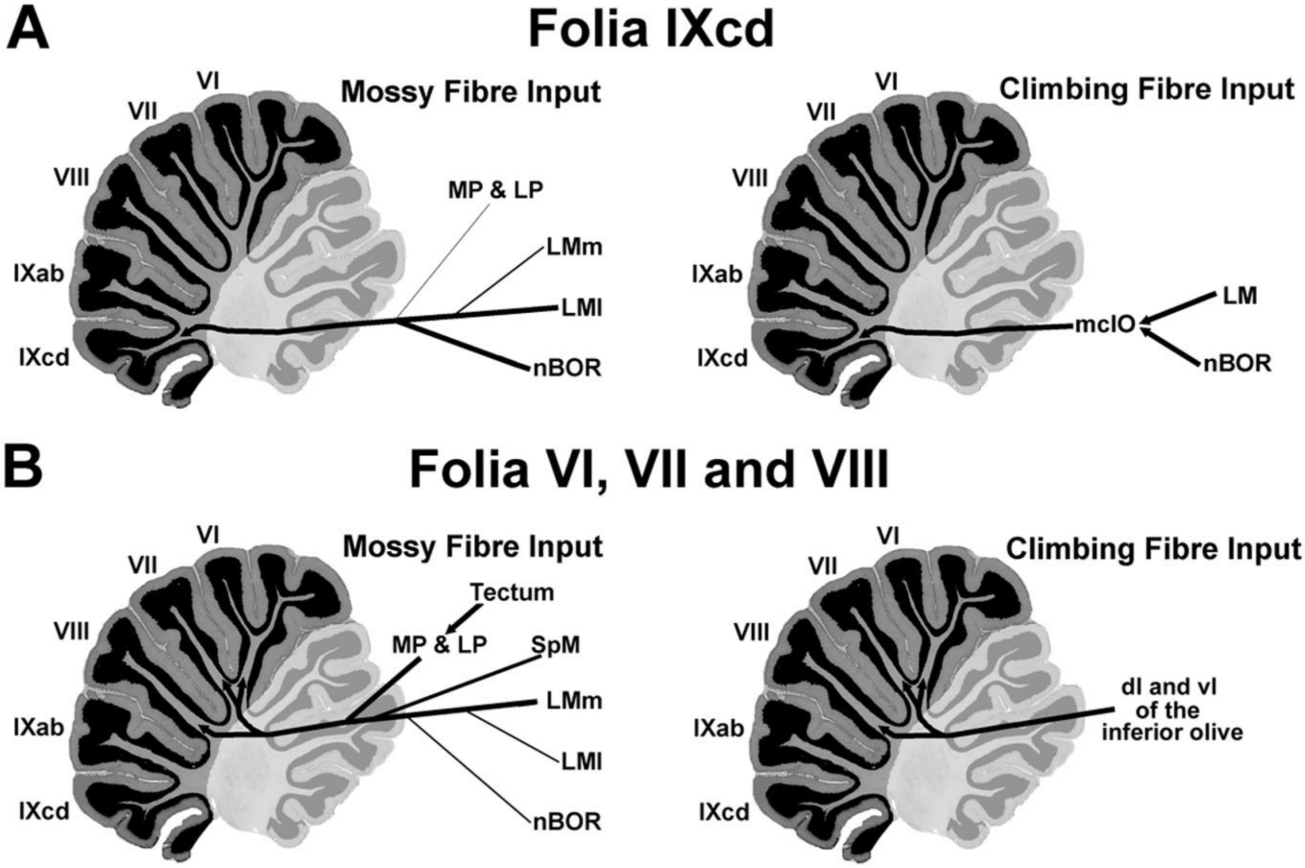

Fig. 7. Visual mossy fiber and climbing fiber pathways to the cerebellum. The thicker lines represent a stronger projection. On a midsagittal section of the pigeon cerebellum, **A** illustrates the mossy fiber (left) and climbing fiber (right) input to folium IXcd. Likewise, **B** illustrates the mossy fiber (left) and climbing fiber (right) input to folia VI–VIII. See text for details. LPC, nucleus laminaris precommisuralis; PPC, nucleus principalis precommisuralis; LMl, lateral subnucleus of the nucleus lentiformis mesencephali; LMm, medial subnucleus of the nucleus lentiformis mesencephali; SpM. medial spiriform nucleus; vl, ventral lamella of the inferior olive; dl, dorsal lamella of the inferior olive; mcIO, medial column of the inferior olive; nBOR, nucleus of the basal optic root.

Larsell (1967) considered the folia of the avian cerebellum to be homologous to those in the vermis of mammals. However, because stem reptiles lack a highly foliated cerebellum, any explicit homology should be viewed with caution. Nonetheless there are striking similarities in folia VI–VIII between birds and mammals. In mammals, VI–VIII is considered the oculomotor cerebellum. There are numerous tectopontine inputs, and they have been implicated in the control and modification of saccades and smooth pursuit eye movements (for review see Voogd and Barmack, 2006). Thus, folia VI–VIII in birds could be involved in the control of saccades. However, this cannot be the sole role of folia VI–VIII. For the mammalian cerebellum, Voogd and Barmack (2006) have emphasized that the term "oculomotor cerebellum" is misleading insofar as the function of this region likely goes beyond oculomotor control. First, only two zones in VII are related to saccades, and the function of the other zones is unknown. Second, the input to folia VI–VIII is multimodal and includes visual, auditory, and trigeminal inputs. Similarly, in birds, there is a heavy trigeminal input to folia VI–VIII (Arends et al., 1984; Arends and Zeigler, 1989), and electrophysiological studies have noted visual, auditory, and somatosensory responses in these folia (Whitlock, 1952; Gross, 1970). These findings suggest that, in both mammals and birds, the function of folia VI–VIII extends beyond oculomotor control.

Proposed role of folia VI–VIII in "steering" behavior

As illustrated in Figure 7B, folia VI–VIII are receiving two types of visual information: optic flow information from LMm and local object motion from a tectopontine system. What is the function of this visual-visual integration? One possible explanation comes from recent work done on area MST of primate cortex. As with pretectal and AOS neurons, MST neurons respond best to large-field stimuli simulating patterns of optic flow (Duffy and Wurtz, 1991), but recent studies of MST have been exploring interactions between optic flow and local motion (Logan and Duffy, 2006). Electrophysiological, psychophysical, and modeling studies have concluded that such optic flow and local motion integration are important for "steering" during locomotion through a complex environment consisting of objects and surfaces (Sherk and Fowler, 2001; Elder et al., 2005; Page and Duffy, 2005; Sato et al., 2005).

Clearly, obstacle avoidance and precise steering would be critical for a variety of behaviors, including flight in birds, and there is some evidence to suggest that folia VI–VIII might be involved in steering. Iwaniuk et al. (2006) showed that folium VI and VII are hypertrophied in bird species that are classified as strong fliers. Hellmann et al. (2004) suggested that the tectopontine projection in pigeons is involved in avoidance. Similarly, Glickstein et al. (1972) implicated pontocerebellar pathways in mammals in the visual control of movement. In general, the tectum is thought to be important for numerous visuomotor behaviors, such as figure–ground segregation and discrimination of the motion of an object from self-induced optical motion (Frost and Nakayama, 1983), orienting responses, and avoidance behavior (Ewert, 1970; Ingle, 1970). Perhaps this tectal information is integrated with optic flow information from LMm in the cerebellum to facilitate obstacle avoidance during locomotion. For example, during translation, a radial optic flow pattern would result, which would be detected by neurons in LMm. In addition, stationary objects would move relative to the background, creating the ideal stimulus to activate deep tectal cells (Frost and Nakayama, 1983), which project to the pontine nuclei (Hellmann et al., 2004). Thus, steering likely involves the integration of multiple visual cues, and the anatomical data found in this study indicate that this integration could be accomplished in folia VI–VIII. Of course, the anatomical information itself does not conclusively validate the function of these folia; however, it does provide the basis for further investigation.

ACKNOWLEDGMENTS

J.M.P.P. was supported by a graduate fellowship from NSERC. We thank Andrew N. Iwaniuk for his assistance.

LITERATURE CITED

Arends J, Voogd J. 1989. Topographic aspects of the olivocerebellar system in the pigeon. Exp Brain Res 17(Suppl):52–57.

Arends JJ, Zeigler HP. 1989. Cerebellar connections of the trigeminal system in the pigeon (*Columba livia*). Brain Res 487:69–78.

Arends JJ, Zeigler HP. 1991. Organization of the cerebellum in the pigeon (*Columba livia*): I. Corticonuclear and corticovestibular connections. J Comp Neurol 306:221–244.

Arends JJ, Woelders-Blok A, Dubbeldam JL. 1984. The efferent connections of the nuclei of the descending trigeminal tract in the mallard (*Anas platyrhynchos* L.). Neuroscience 13:797–817.

Ballas I, Hoffmann KP. 1985. A correlation between receptive field properties and morphological structures in the pretectum of the cat. J Comp Neurol 238:417–428.

Bardy BG, Warren WH Jr, Kay BA. 1999. The role of central and peripheral vision in postural control during walking. Percept Psychophys 61:1356–1368.

Blanks RH, Precht W, Torigoe Y. 1983. Afferent projections to the cerebellar flocculus in the pigmented rat demonstrated by retrograde transport of horseradish peroxidase. Exp Brain Res 52:293–306.

Brecha N, Karten HJ, Hunt SP. 1980. Projections of the nucleus of the basal optic root in the pigeon: an autoradiographic and horseradish peroxidase study. J Comp Neurol 189:615–670.

Buttner-Ennever JA. 2005. The extraocular motor nuclei: organization and functional neuroanatomy. Prog Brain Res 151:95–125.

Buttner-Ennever JA, Horn AK. 1996. Pathways from cell groups of the paramedian tracts to the floccular region. Ann N Y Acad Sci 781:532–540.

Buttner-Ennever JA, Cohen B, Horn AK, Reisine H. 1996a. Pretectal projections to the oculomotor complex of the monkey and their role in eye movements. J Comp Neurol 366:348–359.

Buttner-Ennever JA, Cohen B, Horn AK, Reisine H. 1996b. Efferent pathways of the nucleus of the optic tract in monkey and their role in eye movements. J Comp Neurol 373:90–107.

Cazin L, Magnin M, Lannou J. 1982. Non-cerebellar visual afferents to the vestibular nuclei involving the prepositus hypoglossal complex: an autoradiographic study in the rat. Exp Brain Res 48:309–313.

Clarke PG. 1974. The organization of visual processing in the pigeon cerebellum. J Physiol 243:267–285.

Clarke PG. 1977. Some visual and other connections to the cerebellum of the pigeon. J Comp Neurol 174:535–552.

Cohen B, Reisine H, Yokota JI, Raphan T. 1992. The nucleus of the optic tract. Its function in gaze stabilization and control of visual-vestibular interaction. Ann N Y Acad Sci 656:277–296.

Collewijn H. 1975a. Direction-selective units in the rabbit's nucleus of the optic tract. Brain Res 100:489–508.

Collewijn H. 1975b. Oculomotor areas in the rabbits midbrain and pretectum. J Neurobiol 6:3–22.

Crowder NA, Winship IR, Wylie DR. 2000. Topographic organization of inferior olive cells projecting to translational zones in the vestibulocerebellum of pigeons. J Comp Neurol 419:87–95.

Crowder NA, Lehmann H, Parent MB, Wylie DR. 2003. The accessory optic system contributes to the spatiotemporal tuning of motion-sensitive pretectal neurons. J Neurophysiol 90:1140–1151.

Duffy CJ, Wurtz RH. 1991. Sensitivity of MST neurons to optic flow stimuli. I. A continuum of response selectivity to large-field stimuli. J Neurophysiol 65:1329–1345.

Elder DM, Grossberg S, Mingolla E. 2005. A neural model of visually guided steering, ostacle avoidance, and route selection. Program No. 390.7. Abstract Viewer/Itinerary Planner. Washington, DC: Society for Neuroscience [online].

Ewert JP. 1970. Neural mechanisms of prey-catching and avoidance behavior in the toad (*Bufo bufo* L.). Brain Behav Evol 3:36–56.

Finger TE, Karten HJ. 1978. The accessory optic system in teleosts. Brain Res 153:144–149.

Frost BJ, Nakayama K. 1983. Single visual neurons code opposing motion independent of direction. Science 220:744–745.

Gamlin PD. 2006. The pretectum: connections and oculomotor-related roles. Prog Brain Res 151:379–405.

Gamlin PD, Cohen DH. 1988a. Retinal projections to the pretectum in the pigeon (*Columba livia*). J Comp Neurol 269:1–17.

Gamlin PD, Cohen DH. 1988b. Projections of the retinorecipient pretectal nuclei in the pigeon (*Columba livia*). J Comp Neurol 269:18–46.

Gerrits NM, Epema AH, Voogd J. 1984. The mossy fiber projection of the nucleus reticularis tegmenti pontis to the flocculus and adjacent ventral paraflocculus in the cat. Neuroscience 11:627–644.

Gibson JJ. 1954. The visual perception of objective motion and subjective movement. Psychol Rev 61:304–314.

Gioanni H, Rey J, Villalobos J, Richard D, Dalbera A. 1983. Optokinetic nystagmus in the pigeon (*Columba livia*). II. Role of the pretectal nucleus of the accessory optic system (AOS). Exp Brain Res 50:237–247.

Giolli RA, Blanks RH, Torigoe Y. 1984. Pretectal and brain stem projections of the medial terminal nucleus of the accessory optic system of the rabbit and rat as studied by anterograde and retrograde neuronal tracing methods. J Comp Neurol 227:228–251.

Giolli RA, Blanks RH, Torigoe Y, Williams DD. 1985. Projections of medial terminal accessory optic nucleus, ventral tegmental nuclei, and substantia nigra of rabbit and rat as studied by retrograde axonal transport of horseradish peroxidase. J Comp Neurol 232:99–116.

Giolli RA, Torigoe Y, Blanks RH, McDonald HM. 1988. Projections of the dorsal and lateral terminal accessory optic nuclei and of the interstitial nucleus of the superior fasciculus (posterior fibers) in the rabbit and rat. J Comp Neurol 277:608–620.

Giolli RA, Blanks RH, Lui F. 2006. The accessory optic system: basic organization with an update on connectivity, neurochemistry, and function. Prog Brain Res 151:407–440.

Glickstein M, Stein J, King RA. 1972. Visual input to the pontine nuclei. Science 178:1110–1111.

Gottlieb MD, McKenna OC. 1986. Light and electron microscopic study of an avian pretectal nucleus, the lentiform nucleus of the mesencephalon, magnocellular division. J Comp Neurol 248:133–145.

Graf W, Simpson JI, Leonard CS. 1988. Spatial organization of visual messages of the rabbit's cerebellar flocculus. II. Complex and simple spike responses of Purkinje cells. J Neurophysiol 60:2091–2121.

Gross NB. 1970. Sensory representation within the cerebellum of the pigeon. Brain Res 21:280–283.

Haines DE, Sowa TE. 1985. Evidence of a direct projection from the medial terminal nucleus of the accessory optic system to lobule IX of the cerebellar cortex in the tree shrew (*Tupaia glis*). Neurosci Lett 55:125–130.

Hellmann B, Gunturkun O, Manns M. 2004. Tectal mosaic: organization of the descending tectal projections in comparison to the ascending tectofugal pathway in the pigeon. J Comp Neurol 472:395–410.

Hoffmann KP, Schoppmann A. 1975. Retinal input to direction selective cells in the nucleus tractus opticus of the cat. Brain Res 99:359–366.

Hoffmann KP, Schoppmann A. 1981. A quantitative analysis of the direction-specific response of neurons in the cat's nucleus of the optic tract. Exp Brain Res 42:146–157.

Holstege G, Collewijn H. 1982. The efferent connections of the nucleus of the optic tract and the superior colliculus in the rabbit. J Comp Neurol 209:139–175.

Ilg UJ, Bremmer F, Hoffmann KP. 1993. Optokinetic and pursuit system: a case report. Behav Brain Res 57:21–29.

Ingle D. 1970. Visuomotor functions of the frog optic tectum. Brain Behav Evol 3:57–71.

Ito M, Shiida T, Yagi N, Yamamoto M. 1974. Visual influence on rabbit horizontal vestibulo-ocular reflex presumably effected via the cerebellar flocculus. Brain Res 65:170–174.

Ito M, Jastreboff PJ, Miyashita Y. 1982. Specific effects of unilateral lesions in the flocculus upon eye movements in albino rabbits. Exp Brain Res 45:233–242.

Itoh K. 1977. Efferent projections of the pretectum in the cat. Exp Brain Res 30:89–105.

Iwaniuk AN, Hurd PL, Wylie DRW. 2006. Comparative morphology of the avian cerebellum: II. Size of folia. Brain Behav Evol (in press).

Karten HJ, Finger TE. 1976. A direct thalamo-cerebellar pathway in pigeon and catfish. Brain Res 102:335–338.

Karten H, Hodos W. 1967. A stereotaxic atlas of the brain of the pigeon (*Columba livia*). Baltimore: Johns Hopkins Press.

Kawasaki T, Sato Y. 1980. Afferent projection from the dorsal nucleus of the raphe to the flocculus in cats. Brain Res 197:496–502.

Langer T, Fuchs AF, Scudder CA, Chubb MC. 1985. Afferents to the flocculus of the cerebellum in the rhesus macaque as revealed by retrograde transport of horseradish peroxidase. J Comp Neurol 235:1–25.

Lappe M, Rauschecker JP. 1994. Heading detection from optic flow. Nature 369:712–713.

Larsell O. 1967. The cerebellum: from myxinoids through birds. Jansen J, editor. Minneapolis: The University of Minnesota Press.

Lau KL, Glover RG, Linkenhoker B, Wylie DR. 1998. Topographical organization of inferior olive cells projecting to translation and rotation zones in the vestibulocerebellum of pigeons. Neuroscience 85:605–614.

Lee DN, Lishman R. 1977. Visual control of locomotion. Scand J Psychol 18:224–230.

Lisberger SG, Miles FA, Zee DS. 1984. Signals used to compute errors in monkey vestibuloocular reflex: possible role of flocculus. J Neurophysiol 52:1140–1153.

Lisberger SG, Pavelko TA, Broussard DM. 1994. Neural basis for motor learning in the vestibuloocular reflex of primates. I. Changes in the responses of brain stem neurons. J Neurophysiol 72:928–953.

Logan DJ, Duffy CJ. 2006. Cortical area MSTd combines visual cues to represent 3-D self-movement. Cereb Cortex (in press).

McKenna OC, Wallman J. 1985. Accessory optic system and pretectum of birds: comparisons with those of other vertebrates. Brain Behav Evol 26:91–116.

Miles FA, Lisberger SG. 1981. Plasticity in the vestibulo-ocular reflex: a new hypothesis. Annu Rev Neurosci 4:273–299.

Montgomery N, Fite KV, Bengston L. 1981. The accessory optic system of *Rana pipiens*: neuroanatomical connections and intrinsic organization. J Comp Neurol 203:595–612.

Mustari MJ, Fuchs AF. 1990. Discharge patterns of neurons in the pretectal nucleus of the optic tract (NOT) in the behaving primate. J Neurophysiol 64:77–90.

Nagao S. 1983. Effects of vestibulocerebellar lesions upon dynamic characteristics and adaptation of vestibulo-ocular and optokinetic responses in pigmented rabbits. Exp Brain Res 53:36–46.

Nagao S, Yoshioka N, Hensch T, Hasegawa I, Nakamura N, Nagao Y, Ito M. 1991. The role of cerebellar flocculus in adaptive gain control of ocular reflexes. Acta Otolaryngol Suppl 481:234–236.

O'Brien HL, Tetewsky SJ, Avery LM, Cushman LA, Makous W, Duffy CJ. 2001. Visual mechanisms of spatial disorientation in Alzheimer's disease. Cereb Cortex 11:1083–1092.

Page W, Duffy C. 2005. Cortical neurons reveal perceptual strategies for the active control of steering. Program No. 390.3. Abstract Viewer/Itinerary Planner. Washington, DC: Society for Neuroscience [online].

Pakan JM, Todd KG, Nguyen AP, Winship IR, Hurd PL, Jantzie LL, Wylie DR. 2005. Inferior olivary neurons innervate multiple zones of the flocculus in pigeons (*Columba livia*). J Comp Neurol 486:159–168.

Pakan JM, Krueger K, Kelcher E, Cooper S, Todd KG, Wylie DR. 2006. Projections of the nucleus lentiformis mesencephali in pigeons (*Columba livia*): a comparison of the morphology and distribution of neurons with different efferent projections. J Comp Neurol 495:84–99.

Price NS, Ibbotson MR. 2001. Pretectal neurons optimized for the detection of saccade-like movements of the visual image. J Neurophysiol 85: 1512–1521.

Reiner A, Karten HJ. 1978. A bisynaptic retinocerebellar pathway in the turtle. Brain Res 150:163–169.

Robinson DA. 1976. Adaptive gain control of vestibuloocular reflex by the cerebellum. J Neurophysiol 39:954–969.

Ruigrok TJ. 2003. Collateralization of climbing and mossy fibers projecting to the nodulus and flocculus of the rat cerebellum. J Comp Neurol 466:278–298.

Sato N, Kishore SA, Page W, Vaughn W, Duffy C. 2005. Optic flow and object motion interact in MST neuronal responses. Program No. 390.1. Abstract Viewer/Itinerary Planner. Washington, DC: Society for Neuroscience [online].

Sato Y, Kawasaki T, Ikarashi K. 1983. Afferent projections from the brainstem to the three floccular zones in cats. II. Mossy fiber projections. Brain Res 272:37–48.

Schmidt M. 1996. Neurons in the cat pretectum that project to the dorsal lateral geniculate nucleus are activated during saccades. J Neurophysiol 76:2907–2918.

Sherk H, Fowler GA. 2001. Neural analysis of visual information during locomotion. Prog Brain Res 134:247–264.

Simpson JI. 1984. The accessory optic system. Annu Rev Neurosci 7:13–41.

Simpson JI, Giolli RA, Blanks RH. 1988. The pretectal nuclear complex and the accessory optic system. Rev Oculomot Res 2:335–364.

Srinivasan MV, Poteser M, Kral K. 1999. Motion detection in insect orientation and navigation. Vis Res 39:2749–2766.

Sudkamp S, Schmidt M. 1995. Physiological characterization of pretectal neurons projecting to the lateral posterior-pulvinar complex in the cat. Eur J Neurosci 7:881–888.

Terasawa K, Otani K, Yamada J. 1979. Descending pathways of the nucleus of the optic tract in the rat. Brain Res 173:405–417.

Thielert CD, Thier P. 1993. Patterns of projections from the pontine nuclei and the nucleus reticularis tegmenti pontis to the posterior vermis in the rhesus monkey: a study using retrograde tracers. J Comp Neurol 337:113–126.

Torigoe Y, Blanks RH, Precht W. 1986a. Anatomical studies on the nucleus reticularis tegmenti pontis in the pigmented rat. I. Cytoarchitecture, topography, and cerebral cortical afferents. J Comp Neurol 243:71–87.

Torigoe Y, Blanks RH, Precht W. 1986b. Anatomical studies on the nucleus reticularis tegmenti pontis in the pigmented rat. II. Subcortical afferents demonstrated by the retrograde transport of horseradish peroxidase. J Comp Neurol 243:88–105.

Voogd J, Barmack NH. 2006. Oculomotor cerebellum. Prog Brain Res 151:231–268.

Voogd J, Wylie DR. 2004. Functional and anatomical organization of floccular zones: a preserved feature in vertebrates. J Comp Neurol 470: 107–112.

Voogd J, Gerrits NM, Ruigrok TJ. 1996. Organization of the vestibulocerebellum. Ann N Y Acad Sci 781:553–579.

Waespe W, Cohen B. 1983. Flocculectomy and unit activity in the vestibular nuclei during visual-vestibular interactions. Exp Brain Res 51:23–35.

Waespe W, Henn V. 1987. Gaze stabilization in the primate. The interaction of the vestibulo-ocular reflex, optokinetic nystagmus, and smooth pursuit. Rev Physiol Biochem Pharmacol 106:37–125.

Warren WH Jr, Kay BA, Zosh WD, Duchon AP, Sahuc S. 2001. Optic flow is used to control human walking. Nat Neurosci 4:213–216.

Whitlock DG. 1952. A neurohistological and neurophysiological study of afferent fiber tracts and receptive areas of the avian cerebellum. J Comp Neurol 97:567–635.

Wild JM. 1989. Pretectal and tectal projections to the homologue of the dorsal lateral geniculate nucleus in the pigeon: an anterograde and retrograde tracing study with cholera toxin conjugated to horseradish peroxidase. Brain Res 479:130–137.

Winfield JA, Hendrickson A, Kimm J. 1978. Anatomical evidence that the medial terminal nucleus of the accessory optic tract in mammals provides a visual mossy fiber input to the flocculus. Brain Res 151:175–182.

Winship IR, Wylie DR. 2003. Zonal organization of the vestibulocerebellum in pigeons (*Columba livia*): I. Climbing fiber input to the flocculus. J Comp Neurol 456:127–139.

Winterson BJ, Brauth SE. 1985. Direction-selective single units in the nucleus lentiformis mesencephali of the pigeon (*Columba livia*). Exp Brain Res 60:215–226.

Wylie DR. 2001. Projections from the nucleus of the basal optic root and nucleus lentiformis mesencephali to the inferior olive in pigeons (*Columba livia*). J Comp Neurol 429:502–513.

Wylie DR, Crowder NA. 2000. Spatiotemporal properties of fast and slow neurons in the pretectal nucleus lentiformis mesencephali in pigeons. J Neurophysiol 84:2529–2540.

Wylie DR, Frost BJ. 1993. Responses of pigeon vestibulocerebellar neurons to optokinetic stimulation. II. The 3-dimensional reference frame of rotation neurons in the flocculus. J Neurophysiol 70:2647–2659.

Wylie DR, Frost BJ. 1999. Complex spike activity of Purkinje cells in the ventral uvula and nodulus of pigeons in response to translational optic flow. J Neurophysiol 81:256–266.

Wylie DR, Kripalani T, Frost BJ. 1993. Responses of pigeon vestibulocerebellar neurons to optokinetic stimulation. I. Functional organization of neurons discriminating between translational and rotational visual flow. J Neurophysiol 70:2632–2646.

Wylie DR, Glover RG, Lau KL. 1998a. Projections from the accessory optic system and pretectum to the dorsolateral thalamus in the pigeon (*Columba livia*): a study using both anteretrograde and retrograde tracers. J Comp Neurol 391:456–469.

Wylie DR, Bischof WF, Frost BJ. 1998b. Common reference frame for neural coding of translational and rotational optic flow. Nature 392:278–282.

Wylie DR, Winship IR, Glover RG. 1999. Projections from the medial column of the inferior olive to different classes of rotation-sensitive Purkinje cells in the flocculus of pigeons. Neurosci Lett 268:97–100.

Wylie DR, Brown MR, Winship IR, Crowder NA, Todd KG. 2003a. Zonal organization of the vestibulocerebellum in pigeons (*Columba livia*): III. Projections of the translation zones of the ventral uvula and nodulus. J Comp Neurol 465:179–194.

Wylie DR, Brown MR, Barkley RR, Winship IR, Crowder NA, Todd KG. 2003b. Zonal organization of the vestibulocerebellum in pigeons (*Columba livia*): II. Projections of the rotation zones of the flocculus. J Comp Neurol 456:140–153.

Yakushin SB, Gizzi M, Reisine H, Raphan T, Buttner-Ennever J, Cohen B. 2000. Functions of the nucleus of the optic tract (NOT). II. Control of ocular pursuit. Exp Brain Res 131:433–447.

Yamada J, Noda H. 1987. Afferent and efferent connections of the oculomotor cerebellar vermis in the macaque monkey. J Comp Neurol 265:224–241.

Zee DS, Yamazaki A, Butler PH, Gucer G. 1981. Effects of ablation of flocculus and paraflocculus of eye movements in primate. J Neurophysiol 46:878–899.